Spurious Radiation From a Practical Source on a Covered Microstrip Line

William L. Langston, *Student Member, IEEE,* Jeffery T. Williams, *Senior Member, IEEE,* David R. Jackson, *Fellow, IEEE,* and Francisco Mesa, *Member, IEEE*

***Abstract*—The TM_0 parallel-plate mode field that is radiated from the currents induced on a covered microstrip transmission line by a finite-gap voltage source is studied. The behavior of the total radiation field (the field radiated by the total strip current) is investigated, along with the field radiated by the constituent current components that make up the total current, namely the bound-mode (BM) and continuous-spectrum currents. The continuous-spectrum current is further resolved into the sum of a physical leaky-mode current and a residual-wave current, and the fields radiated by each of these separate components are examined. It is determined that leaky-mode fields can contribute to crosstalk and other interference effects near the source and within an angular leakage region, while the radiation field from the BM current is the predominant mechanism for these effects further away from the gap source, outside the leakage region. The field radiated from the residual-wave current can be quite strong in the "spectral-gap region," which is the frequency region where the leaky mode is nonphysical, and therefore the leaky mode does not contribute directly to the spectrum of current on the strip in the decomposition used here.**

***Index Terms*—Crosstalk, leaky waves, microstrip, microwave integrated circuits, printed circuits, radiation.**

I. Introduction

THE existence of leaky modes on printed-circuit transmission lines has recently been the subject of considerable interest [1]–[14]. These modes are undesirable since they result in increased attenuation of the signal and can result in crosstalk with adjacent circuit components and other spurious effects, including interference with bound modes (BMs) that also propagate on the line. Of particular interest is the existence of leaky dominant modes on the structure. A dominant leaky mode is one in which the current distribution on the conducting strip closely resembles that of the bound quasi-TEM mode of propagation. Therefore, such a leaky mode is expected to be strongly excited by a customary feed. Leaky dominant modes have been found on a number of planar transmission-line structures including multilayer stripline structures [1], microstrip lines with isotropic and anisotropic substrates [2], [3], coplanar strips [4], slotline [5], and coplanar waveguides [5], [6].

Manuscript received March 30, 2001; revised August 23, 2001. This work was supported in part by the State of Texas under the Advanced Technology Program. The work of F. Mesa was supported in part by the Spanish Comisión Interministerial de Ciencia y Tecnología under Project TIC98-0630.

W. L. Langston, J. T. Williams, and D. R. Jackson are with the Department of Electrical and Computer Engineering, University of Houston, Houston, TX 77204-4005 USA (e-mail: djackson@uh.edu).

F. Mesa is with the Department of Applied Physics 1, University of Seville, Seville 41012, Spain.

Publisher Item Identifier S 0018-9480(01)10475-8.

More recently, theoretical work has focused on studying the current on stripline and microstrip structures due to excitation from a small, finite-length gap feed on the line [7]. It was shown that the total current on the strip excited by the source can be decomposed into the sum of the well-known BM current and a continuous-spectrum current. The continuous- spectrum current was further decomposed into the sum of all physical leaky-mode currents and a *residual-wave* current. The residual-wave current is simply that component of the continuous-spectrum current that is not a part of the leaky-mode currents. It was demonstrated that spurious transmission effects can result due to the interference of the BM and the continuous-spectrum currents even when a leaky mode is not physical. When a leaky mode is physical, very significant spurious effects can be observed.

This work presents the calculation of the *fields* radiated by the BM, leaky-mode, and residual-wave currents excited by a finite source on covered microstrip transmission lines. The radiation is into the dominant TM_0 parallel-plate mode of the covered structure. These radiated fields allow issues associated with crosstalk between adjacent transmission lines and other circuit elements to be meaningfully addressed. Results will be presented for four cases that have the following strip current characteristics: 1) a BM and a predominant leaky-mode current; 2) a BM together with leaky-mode and residual-wave currents that are comparable in magnitude; 3) a BM together with a strong residual-wave current, with no physical leaky mode; and 4) a BM with a weak residual-wave current and no physical leaky mode. These cases facilitate a greater understanding of the role of the residual wave by isolating its effects from those of the physical leaky mode.

In the latter two cases, the leaky mode is inside the spectral-gap region [8], where it is a slow wave with respect to the TM_0 parallel-plate mode. The convenient calculation procedure employed here assumes that the leaky mode is completely nonphysical within this region, and therefore does not explicitly appear in the current spectrum on the strip, as discussed in detail in [11].

II. Summary of Analysis

A. Constituent Currents on the Strip Due to a Practical Source

A diagram of the covered microstrip structure (two-layer stripline) with a small but finite gap source is shown in Fig. 1. The conducting strip is assumed to be infinite in the $\pm z$ directions and all of the conductors are assumed to be perfect conductors. For simplicity, the strip width W is assumed to be

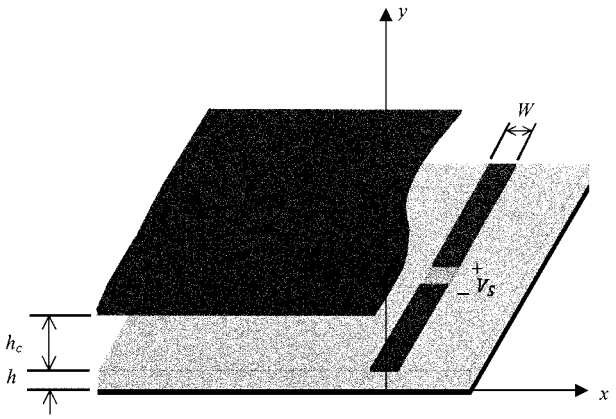

Fig. 1. Covered microstrip structure with a small, finite-length gap source.

small so that the transverse component of the current can be neglected. Therefore, the surface current on the strip is given by

$$J_z(x, z) = I(z)\eta(x) \tag{1}$$

where $\eta(x)$ is the normalized transverse shape function for the strip current $I(z)$ taken as [7]

$$\eta(x) = \frac{1}{\pi\sqrt{(W/2)^2 - x^2}}. \tag{2}$$

An electric field integral equation for the unknown strip current is developed assuming the field for the gap source is a pulse of the form

$$E_{\mathrm{GAP}}(z) = \frac{1}{\Delta}, \qquad |z| < \Delta/2 \tag{3}$$

where Δ is an effective gap width, taken to be $0.05\lambda_0$ in this study. The Galerkin method in the spectral domain is then used to solve the electric field integral equation [7]. This results in a closed-form solution for the Fourier transform of the current $I(z)$ on the strip, due to the gap source [7]. The result is

$$\tilde{I}(k_z) = \frac{2\pi\,\tilde{E}_{\mathrm{GAP}}(k_z)}{\displaystyle\int_{C_x} \tilde{G}_{zz}(k_x, k_z, h)\,\tilde{\eta}^2(k_x)\,dk_x} \tag{4}$$

where $\tilde{G}_{zz}$ is the $\hat{\mathbf{z}}\hat{\mathbf{z}}$ component of the spectral-domain dyadic electric-field Green's function at $y = h$, and $\tilde{\eta}$ and $\tilde{E}_{\mathrm{GAP}}$ are the Fourier transforms of the transverse profile of the strip current density and the electric field in the gap in the x and z directions, respectively [7]. The strip current is then found by an inverse transform, yielding

$$I(z) = \frac{1}{2\pi}\int_{C_Z} \tilde{I}(k_z)e^{-jk_z z}\,dk_z \tag{5}$$

where C_Z is the Sommerfeld-type path shown in Fig. 2(a).

The total current in (5) may be decomposed by suitably deforming the path of integration in the k_z-plane (Fig. 2). The k_z-plane has branch points at $\pm k_{pp}$, where k_{pp} is the propagation wavenumber of any of the parallel-plate modes inside the layered structure. Assuming that only the TM_0 parallel-plate mode is above cutoff, there will be a pair of branch points at $\pm k_{\mathrm{TM}_0}$ on the real axis, where k_{TM_0} is the wavenumber of the dominant TM_0 parallel-plate mode of the layered structure. All other branch points will lie on the imaginary axis. (The branch points are discussed further in [7].) A pole also lies on the positive real axis, at the wavenumber of the BM that propagates on the covered microstrip line. If the original path in Fig. 2(a) is deformed around the TM_0 branch cut, as shown in the figure, the total current can be expressed as the sum of the residue contribution from the BM pole—the BM current—and the contribution from the integral around the branch cuts in the lower half-plane—the continuous-spectrum current [9], [10]. Further, as shown in Fig. 2(b), the branch-cut integral can be deformed to a path that encloses all of the branch cuts along the negative imaginary axis and a vertical steepest descent path that encloses the TM_0 branch point [11]. In this way, the continuous-spectrum current can be further decomposed. This decomposition is into leaky-mode currents due to the residues of any leaky-mode poles that are captured in the physical region of the k_z-plane (the region between the imaginary axis and the vertical steepest descent path, where the leaky modes are fast waves with respect to the TM_0 parallel-plate mode), plus a residual term (residual-wave current) coming from the steepest descent path accounting for that part of the continuous spectrum that is not well represented by the leaky-mode currents. Further details are discussed in [11], [12], and particularly in [11] where the vertical steepest decent path is described.

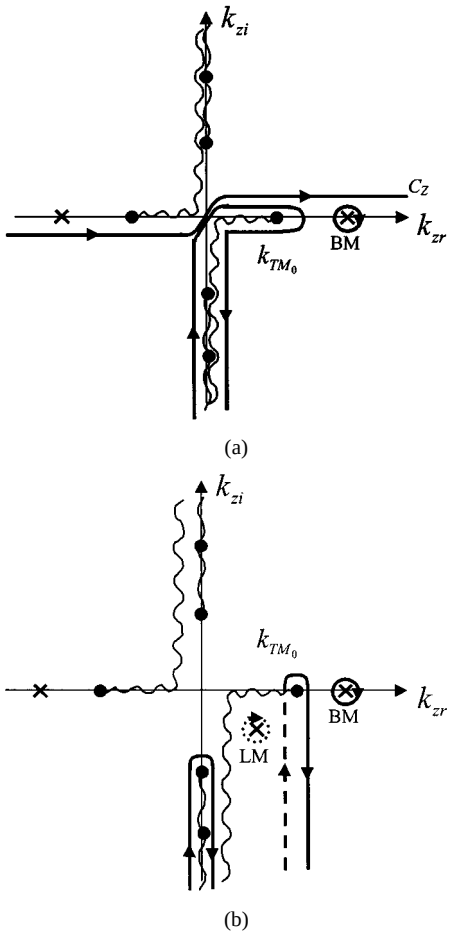

Fig. 2. Complex k_z-plane showing: (a) the original path of integration used to calculate the total strip current and (b) the deformed path used to decompose the total strip current into the BM, leaky-mode, and residual-wave components.

The BM current on the line due to the gap source has the familiar form

$$I_{\mathrm{BM}}(z) = A_{\mathrm{BM}}\, e^{-j\, k_z^{\mathrm{BM}}|z|} \tag{6}$$

where A_{BM} is the BM excitation coefficient and for lossless structures k_z^{BM} is a purely real number. Similarly, the leaky-mode current launched from the source has the form

$$I_{\mathrm{LM}}(z) = A_{\mathrm{LM}}\, e^{-j\, k_z^{\mathrm{LM}}\,|z|} \tag{7}$$

where A_{LM} is the leaky-mode excitation coefficient and k_z^{LM} is, in general, a complex number ($k_z^{\mathrm{LM}} = \beta_z^{\mathrm{LM}} - j\,\alpha_z^{\mathrm{LM}}$). The residual-wave current does not have a closed-form expression; however, asymptotically (for large z), it has the form [11]

$$I_{\mathrm{RW}}(z) \sim A_{\mathrm{RW}}\, \frac{e^{-j\, k_{\mathrm{TM}_0}\,|z|}}{(k_{\mathrm{TM}_0}|z|)^{3/2}} \tag{8}$$

where A_{RW} is the residual-wave excitation coefficient.

B. TM_0-*Mode Fields Due to the Strip Currents*

Once determined, the strip currents can be used to find the fields radiated by the line and the feed. Assuming that only the TM_0 parallel-plate mode is above cutoff in the background structure, the fields radiated into this parallel-plate mode by the strip current can be formulated in terms of the fields radiated into this mode by a z-directed infinitesimal electric dipole, by integrating over the strip current. The vertical parallel-plate mode electric field radiated from the unit-amplitude dipole is

$$E_y(x, y, z) = A\, f(y) H_1^{(2)}(k_{\mathrm{TM}_0}\rho)\cos(\phi) \tag{9}$$

where A is a constant that can be determined by spectral-domain methods (see the Appendix), ρ and ϕ denote cylindrical coordinates (with ϕ measured from the z axis), and

$$f(y) = \begin{cases} \cos(k_{y1}y), & y < h \\ \dfrac{\varepsilon_r \cos(k_{y1}h)}{\cos(k_{y0}h_c)}\cos(k_{y0}(h + h_c - y)), & y > h \end{cases} \tag{10}$$

with

$$k_{y1} = \sqrt{\varepsilon_r k_0^2 - k_{\mathrm{TM}_0}^2} \quad \text{and} \quad k_{y0} = \sqrt{k_0^2 - k_{\mathrm{TM}_0}^2}.$$

The function $f(y)$ is a normalized function that describes the vertical variation of the fields of the parallel-plate mode inside the structure. Integrating over the strip current, the result is

$$E_y(x, y, z) = A\, f(y) \int_{-\infty}^{\infty}\int_{-W/2}^{W/2} \cdot I(z')\eta(x') H_1^{(2)}(k_{\mathrm{TM}_0}\rho')\cos\phi'\, dx'\, dz' \tag{11}$$

where

$$\rho' = \sqrt{(x - x')^2 + (z - z')^2}$$

$$\phi' = \tan^{-1}\left[\frac{x - x'}{z - z'}\right].$$

In the case of the covered-microstrip structure of Fig. 1, a spectral-domain analysis yields (see the Appendix for a derivation and explanation of the notation)

$$A = \frac{k_{\mathrm{TM}_0}^2\, \mathrm{Res}\{V_i^{\mathrm{TM}}(k_{pp})\}}{j\, 2\, k_{y1}\sin(k_{y1}h)}. \tag{12}$$

For simplicity, the width W of the microstrip line is assumed to be small. Hence, collapsing the width of the microstrip line to $x' = 0$, the double integral for the fields simplifies to

$$E_y(x, y, z) = A\, f(y) \int_{-\infty}^{\infty} I(z') H_1^{(2)}(k_{\mathrm{TM}_0}\rho')\cos\phi'\, dz'. \tag{13}$$

The substrate voltage V_h will be plotted for the results presented in this paper. The substrate voltage corresponds, qualitatively, to the *crosstalk* signal that would be impressed upon a circuit component at a given location. The substrate voltage is calculated using

$$V_h = -\int_0^h E_y\, dy. \tag{14}$$

Since the only part of the vertical electric field that varies with respect to y is $f(y)$, the substrate voltage becomes

$$V_h(x, z) = -A\, h\, \mathrm{sinc}(k_{y1}\, h) \cdot \int_{-\infty}^{\infty} I(z') H_1^{(2)}(k_{\mathrm{TM}_0}\rho')\cos\phi'\, dz' \tag{15}$$

with

$$\mathrm{sinc}(x) \equiv \frac{\sin(x)}{x}.$$

The numerical integration of (15) is slowly convergent, especially for the lossless BM current. Thus, the Shanks transformation is used to improve the convergence rate of the numerical integration by eliminating the most pronounced transient behavior from the integrand as z' becomes large. In general, the Shanks transformation improves the convergence of a sequence of partial sums whose nth term takes the form

$$\Sigma_n = \Sigma + \alpha q^n \tag{16}$$

where $|q| < 1$; hence, $\Sigma_n \to \Sigma$ as $n \to \infty$ [15]. For such a sequence of partial sums, the nonlinear Shanks transformation

$$S(\Sigma_n) = \frac{\Sigma_{n+1}\,\Sigma_{n-1} - \Sigma_n^2}{\Sigma_{n+1} + \Sigma_{n-1} - 2\,\Sigma_n} \tag{17}$$

creates a new, more rapidly convergent sequence $S(\Sigma_n)$ [15]. The numerical integration of (15) converges very rapidly when an iterated Shanks transformation is initiated at the nominal location $z' = L$, where L is equal to the greater of either twice the maximum radial observation distance $\rho = \sqrt{x^2 + z^2}$ or $100\lambda_0$. Applying the Shanks transformation at this location allows the partial sum created by the numerical integration of (15) to approach the asymptotic form of (16), for which the Shanks transformation is applicable. Hence, the numerical integration for $z' > L$ is greatly accelerated.

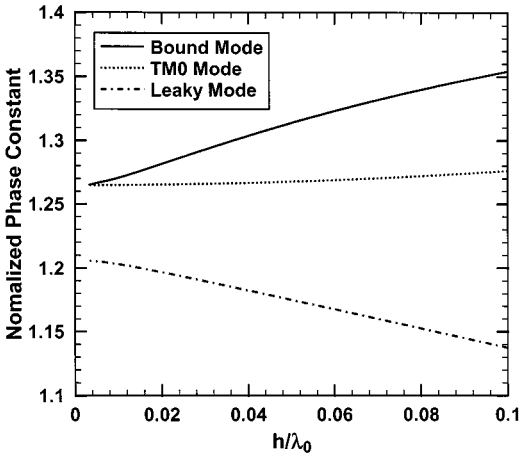

Fig. 3. Dispersion plot showing the normalized phase constants β/k_0 versus normalized frequency h/λ_0 for a covered microstrip ($h_c = 0.455\,h$, $W = h$, and $\varepsilon_r = 2.2$).

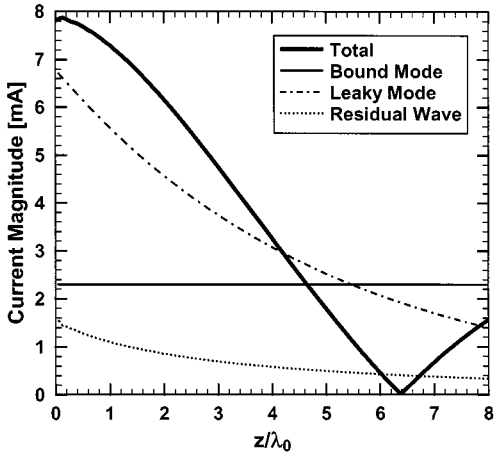

Fig. 4. Strip current magnitude for a covered microstrip ($h = 0.02\,\lambda_0$, $h_c = 0.455\,h$, $W = h$, and $\varepsilon_r = 2.2$) with a 1-[V] gap source.

III. Results

All of the cases presented in this paper consider a covered microstrip with $W = h$ and relative permittivity of the dielectric substrate $\varepsilon_r = 2.2$. The first case examined is that of a covered microstrip with substrate thickness $h = 0.02\,\lambda_0$ and cover height $h_c = 0.455\,h$. The dispersion plot in Fig. 3 shows that the low cover height of this structure allows a physical leaky mode to exist at *all* frequencies. It also illustrates the relationship between the phase constants of the bound and leaky modes, and the TM_0 parallel-plate mode. For $h/\lambda_0 = 0.02$, $k_z^{\mathrm{BM}} = 1.281\,k_0$, $k_z^{\mathrm{LM}} = (1.97 - j0.0315)\,k_0$, and $k_{\mathrm{TM}_0} = 1.265\,k_0$. For this specific covered microstrip, the leaky mode is very strong [12]. This is clearly demonstrated by observing the strip current for this structure in Fig. 4. As shown in this figure, the leaky-mode current excited by the gap source is significantly stronger than that for the BM for distances less than 5.5 wavelengths from the source. In fact, for this case, the interference between the BM and continuous-spectrum (dominated by the leaky mode) currents results in a complete transmission null on the line near $z = 6.4\,\lambda_0$[12].

Figs. 5–7 show plots of the normalized substrate voltage versus longitudinal distance z at $x = 0.1\lambda_0$, λ_0, and $4\lambda_0$, respectively. In all cases, the radiation field is zero at $z = 0$ due to the symmetry of the gap-source excitation, which causes the current to be an even function of z' in (15).

As expected, these results clearly demonstrate strong radiation fields associated with the leaky-mode current on the strip.

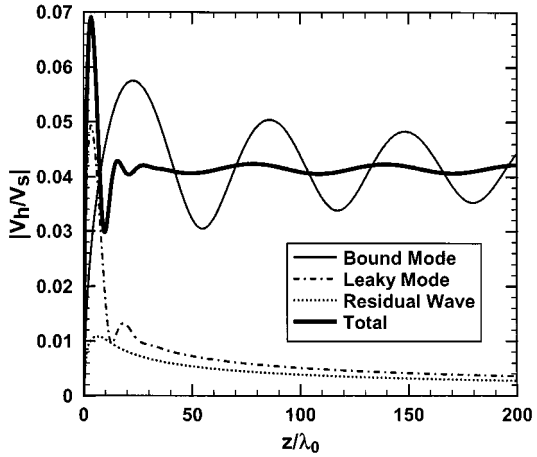

Fig. 5. Normalized substrate voltage for the covered microstrip of Fig. 4 at $x = 0.1\,\lambda_0$.

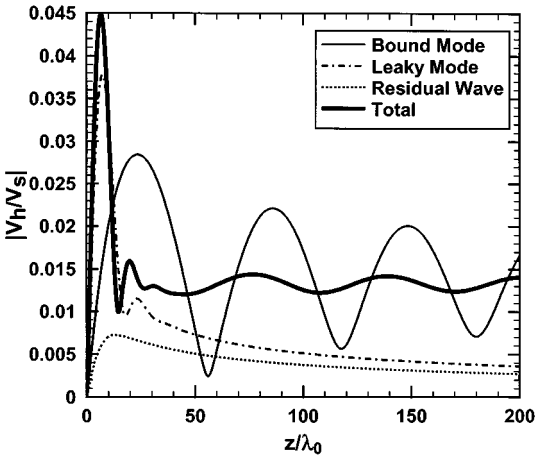

Fig. 6. Normalized substrate voltage for the covered microstrip of Fig. 4 at $x = \lambda_0$.

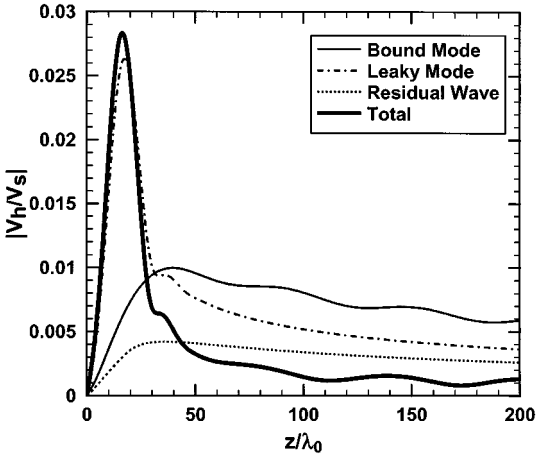

Fig. 7. Normalized substrate voltage for the covered microstrip of Fig. 4 at $x = 4\,\lambda_0$.

The leaky-mode radiation field is very strong in the region near the gap feed, and a large peak is observed near to, but less than, the value of z predicted by the leakage angle ($\phi \simeq 18.9°$). The shift between the actual and predicted peak locations will be explained presently. Relative to the other radiation fields, the leaky-mode field at the peak becomes stronger as the transverse distance (x) away from the strip increases. This effect can be explained qualitatively by geometrical optics [16]. Geometrical optics predicts that the peak leaky-mode field is constant along the angle of leakage, whereas the other field components decrease in magnitude as the radial distance from the source increases. Another observation is that, as x is increased, the leaky-mode fields extend over a wider range of z. (Note that, in the far field, the broadening of the leaky-mode pattern is directly proportional to x since the far-field pattern shape is only a function of ϕ. The radiated fields in Figs. 5–7 have not yet reached the far-field limit; however this broadening is already evident.)

Surprisingly, the BM field radiated from the strip is also strong away from the line. The BM field can be physically interpreted as the sum of two fields. The first field is that from an infinite BM line current along the strip (the BM near field), which produces fields that decay exponentially from the strip. The second field is that which is radiated as a result of the slope discontinuity in the BM current at the gap source. The slope discontinuity corresponds to the fact that the derivative of the BM current in (6) is discontinuous at the source. The oscillations in the BM field in Figs. 5 and 6 are a result of the interference between the fields associated with these two mechanisms. The source-discontinuity radiation propagates with the wavenumber of the dominant mode of the background structure (k_{TM_0}). Thus, the period of the oscillations is well predicted by the difference between the phase constants of the two propagating waves that contribute to the BM radiation field, as

$$\lambda_{\mathrm{int}}^{\mathrm{BM}} = \frac{2\pi}{k_z^{\mathrm{BM}} - k_{\mathrm{TM}_0}}. \tag{18}$$

The BM interference pattern follows a distinct pattern as x is increased. Close to the line, for small x, the infinite-line BM field dominates the interference pattern amplitude and this field is modulated by the BM source-discontinuity radiation. Hence, the field shows oscillations about an essentially fixed average level. Also notice in Fig. 5 that the oscillations in the total radiation field are much weaker in amplitude compared to those of the BM field by itself. The fields radiated by the leaky-mode and residual-wave currents destructively interfere with the BM source-discontinuity radiation reducing the overall interference level in the total field. As the transverse distance is increased, the field of the infinite-line BM decays more rapidly than that of the BM source-discontinuity field, and the roles of the two BM field components begin to reverse. That is, the BM field for larger x resembles that of the BM discontinuity radiation, modulated by the field of the infinite BM current. Fig. 7 shows the result of this transition.

The oscillations in the total field in Fig. 7 are similar in amplitude and period to those in the BM field, but the level of the total field is lower than that of the BM. Thus, the destructive interference with the continuous-spectrum (leaky-mode and residual-wave) radiation reduces the overall average level of the field. Eventually, the BM interference disappears as the transverse distance from the strip becomes large, due to the exponential decay of the infinite-line BM near field, which is governed by

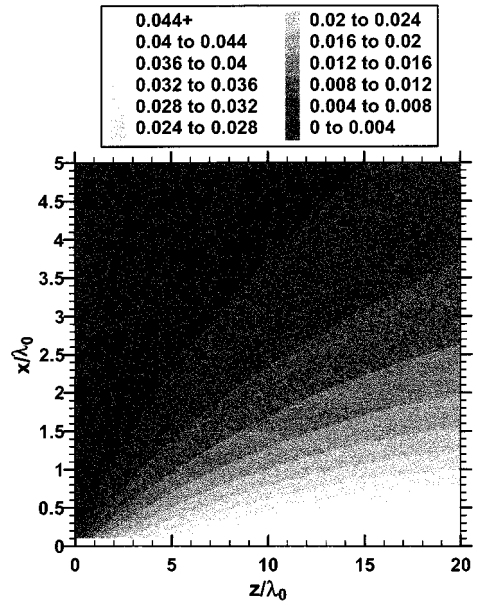

Fig. 8. Normalized substrate voltage (BM) for the covered microstrip of Fig. 4.

$$\alpha_x = \sqrt{(k_z^{\mathrm{BM}})^2 - k_{\mathrm{TM}_0}^2}. \tag{19}$$

In this example, however, this decay is relatively slow since the BM propagates with a phase constant that is only slightly larger than that of the TM_0 parallel-plate mode ($k_z^{\mathrm{BM}} = 1.281\,k_0$, $k_{\mathrm{TM}_0} = 1.265\,k_0$). Thus, the oscillations in the BM field do not completely disappear until x is approximately 4–$5\lambda_0$.

For large z, the leaky-mode current has been essentially radiated; as a result, the BM field is predominant in this region. Furthermore, Fig. 7 clearly shows that, for large z, the leaky-mode and residual-wave fields generally destructively interfere with the BM fields, causing the total field to have a similar appearance to that of the leaky mode near the leakage angle and significantly lower fields elsewhere.

The contour plots in Figs. 8–10 show the behavior of the radiated fields in a region relatively close to the gap source. In these figures, the radiation near the source due to each of the individual current components is shown. Figs. 8 and 10 show that the BM and the residual-wave radiation fields have similar end-fire shapes. The BM radiation field does not reflect the BM oscillations seen in Figs. 5–7 due to the relatively large period of these oscillations, and the plotting scale used in Fig. 8. Fig. 9 shows the leaky-mode radiation propagating away from the line about a specific angle of leakage, and this leakage field is strong. It is interesting to note that the peak leakage field is not at the source, but rather down the line from the source. That is, the leaky-mode field requires a certain distance to become "well-formed." Measured from this point, the observed angle of leakage closely matches the classically predicted leakage angle ($\phi \simeq 18.9°$). This shift in the effective radiation center of the

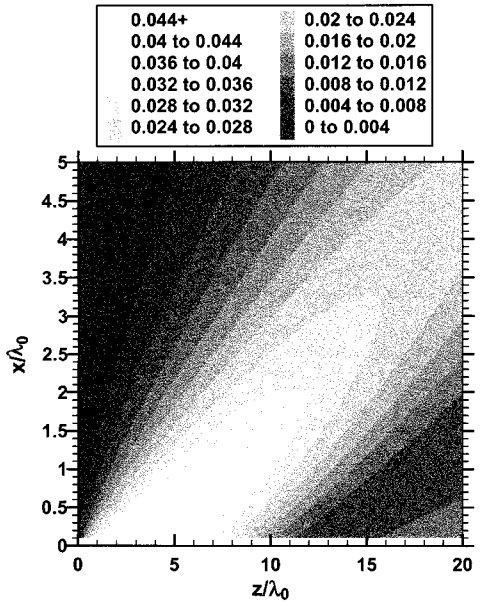

Fig. 9. Normalized substrate voltage (leaky mode) for the covered microstrip of Fig. 4.

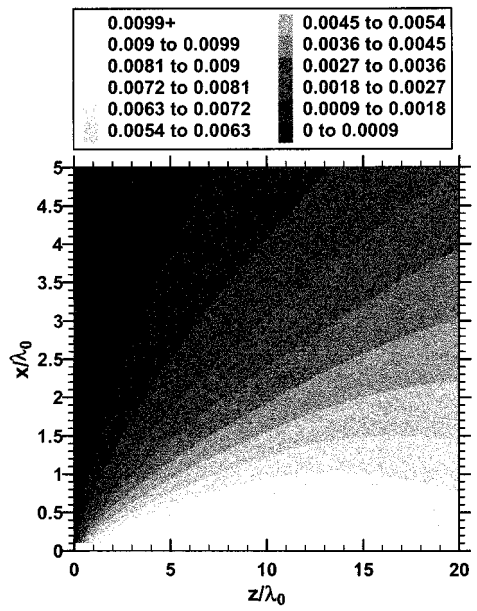

Fig. 10. Normalized substrate voltage (residual wave) for the covered microstrip of Fig. 4.

leaky mode explains the location of the leaky-mode peaks in Figs. 5–7.

Fig. 11 shows the magnitude of the total field for this structure, obtained by summing the complex fields in Figs. 8–10. It can be readily seen that the leaky-mode field dominates the total field near the source and close to the leakage angle, while the BM field dominates the total field near the strip for larger z.

One method of quantifying the energy lost to radiation is to calculate the BM efficiency, defined as

$$e_{\mathrm{BM}} \equiv \frac{P_{\mathrm{BM}}}{P_{\mathrm{Total}}} = \frac{Z_0 \left|I_{\mathrm{BM}}\right|^2}{\frac{1}{2}\,\mathrm{Re}\{I_{\mathrm{Total}}(0)\}} \tag{20}$$

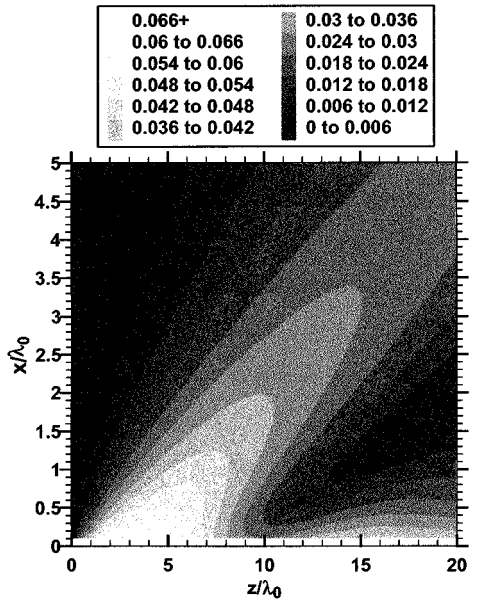

Fig. 11. Normalized substrate voltage (total) for the covered microstrip of Fig. 4.

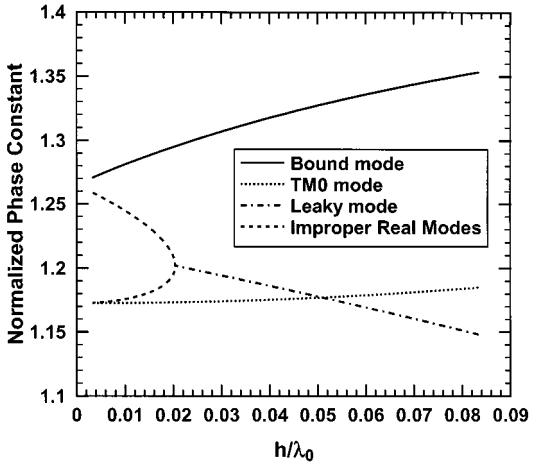

Fig. 12. Dispersion plot showing the normalized phase constants β/k_0 versus normalized frequency h/λ_0 for a covered microstrip ($h_c = h$, $W = h$, and $\varepsilon_r = 2.2$).

where P_{BM} is the power propagating in the BM in both directions along the line and P_{Total} is the total power provided by the 1-[V] gap source. Performing this calculation for this structure using Ansoft HFSS to calculate Z_0 for the BM, it is found that $e_{\mathrm{BM}} = 7.3\%$. Hence, 92.7% of the source power is lost to radiation, both by the radiating leaky-mode current and by the source-discontinuity radiation from the different current components. This reinforces the assertion that this particular covered microstrip is subject to significant power loss when used within a practical microwave integrated circuit, which is an important design consideration [13], [14].

For the remaining cases, a covered microstrip with $h_c = h$, $\varepsilon_r = 2.2$, and $W = h$ will be considered. Fig. 12 shows the dispersion plot for this structure. This figure illustrates three distinct regions of behavior. In the first region ($h/\lambda_0 > 0.052$), a physical leaky mode exists. In the second region ($0.021 < h/\lambda_0 < 0.052$), a leaky mode exists but is in the nonphysical

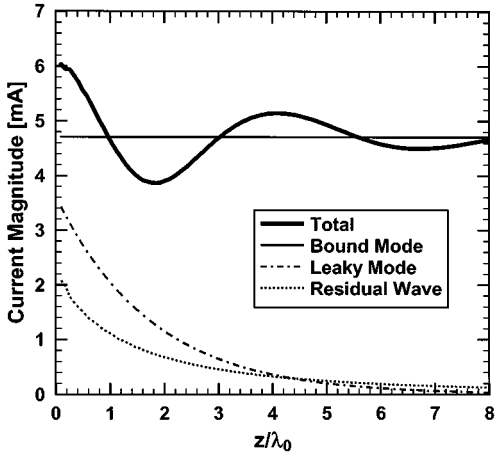

Fig. 13. Strip current magnitude for a covered microstrip ($h = 0.08\,\lambda_0$, $h_c = h$, $W = h$, and $\varepsilon_r = 2.2$) with a 1-[V] gap source.

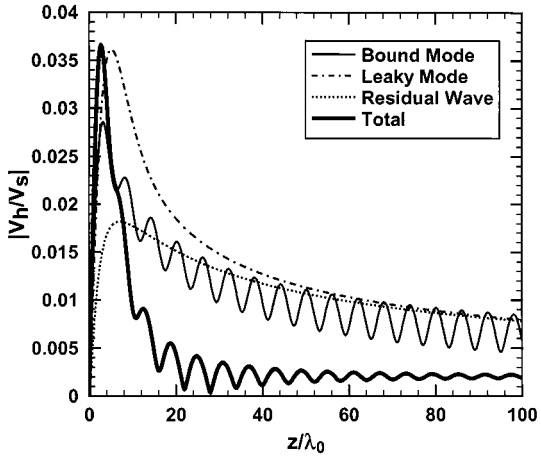

Fig. 14. Normalized substrate voltage for the covered microstrip of Fig. 13 at $x = \lambda_0$.

spectral-gap region. In this region, the calculation method that is used here predicts no physical leaky-mode current [because the leaky-mode pole is not captured by the steepest descent deformation in Fig. 2(b)]. However, the leaky-mode pole influences the residual-wave current and thus makes an indirect contribution to the strip current. In the third region ($h/\lambda_0 < 0.021$), there is no leaky mode, only a pair of nonphysical real-improper modes. This paper will examine one case from each of these regions.

The first case presented is a case where there is physical leakage ($h = 0.08\,\lambda_0$). Fig. 13 shows the current components excited for this case. In this example, the leaky-mode and residual-wave currents are excited with similar amplitudes. The figure also illustrates how the leaky-mode and residual-wave currents interfere with the BM current to cause oscillations in the total current.

Fig. 14 shows the normalized substrate voltage parallel to the line at $x = \lambda_0$. The higher frequency ($h = 0.08\,\lambda_0$) causes the leaky-mode and residual-wave fields in this case to be quite strong for larger values of z, in comparison with Fig. 6 from the previous case. The BM oscillations have a much smaller period than in Fig. 6, but this fact is easily explained by the larger separation between the BM and the TM_0 parallel-plate mode phase

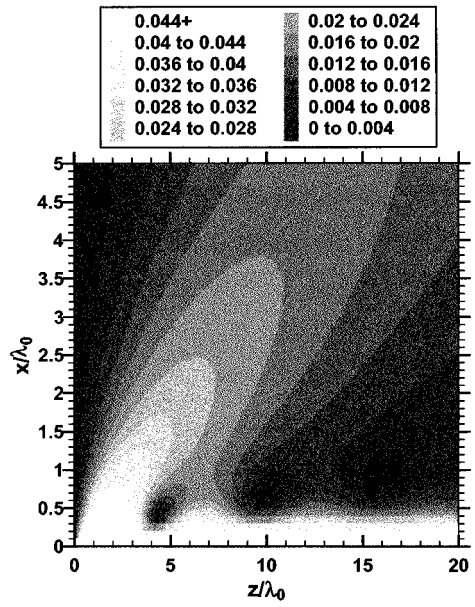

Fig. 15. Normalized substrate voltage (total) for the covered microstrip of Fig. 13.

constants. This larger separation also explains the lower relative magnitude of the oscillations in the BM field at this transverse distance, since α_x is larger [see (19)]. For this structure, the BM source-discontinuity radiation is stronger than the field of the infinite BM current at this transverse distance. Hence, the infinite-line BM field is acting as the modulator of the BM discontinuity radiation in this case. The contour plot shown in Fig. 15 presents the total radiation field for this case. Similar to the predominant leaky-mode case (Fig. 11), the primary radiation away from the line exists around a leakage angle ($\phi \simeq 13.6°$). However, in this case, the leakage angle is not as well defined as in Fig. 11. The apexes of the contours for the total radiation in the leakage region bend inward toward the line. This curvature of the leakage angle appears as a result of the relatively strong residual-wave and BM source-discontinuity radiation. Several periods of the BM interference pattern are apparent along the longitudinal dimension of the line in this figure. The inclusion of this BM interference pattern completes the general picture of the total radiated fields for the instance when all three current components are strongly excited.

When the frequency is decreased so that the leaky-mode pole is no longer captured in the spectral integration of the current, the leaky mode becomes nonphysical [11]. The leaky mode is then said to be in the spectral-gap region [8], corresponding to $\beta_z^{LM} > k_{\mathrm{TM}_0}$. In this case, the continuous-spectrum current consists entirely of the residual-wave current. The next example corresponds to such a case. The normalized substrate height for this case is $h/\lambda_0 = 0.04$ (see Fig. 12), and the corresponding current is detailed in Fig. 16. Similar to the previous case, the superposition of the lossless BM current and the decaying continuous-spectrum (purely residual-wave) current creates an oscillatory total current.

The resulting normalized substrate voltage at $x = \lambda_0$ is shown in Fig. 17. Once again, the infinite-line BM field is modulating the BM source-discontinuity radiation field. Since in this case there is not the added complexity of having leaky-

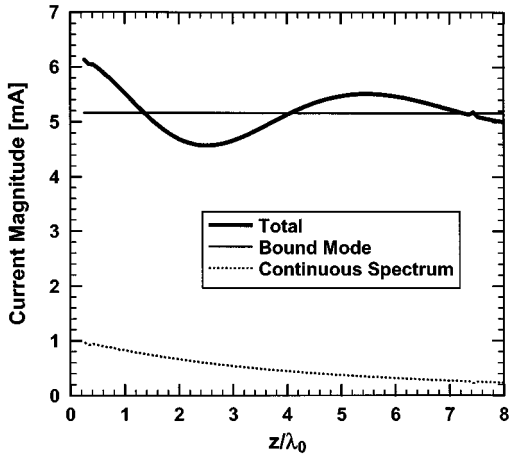

Fig. 16. Strip current magnitude for a covered microstrip ($h = 0.04\,\lambda_0$, $h_c = h$, $W = h$, and $\varepsilon_r = 2.2$) with a 1-[V] gap source.

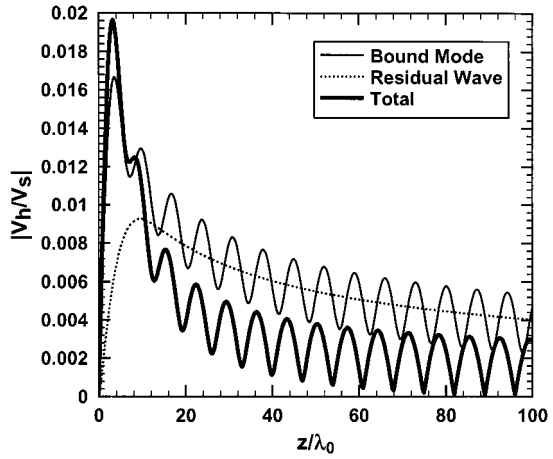

Fig. 17. Normalized substrate voltage for the covered microstrip of Fig. 16 at $x = \lambda_0$.

mode radiation, this plot illustrates the destructive interference between a residual wave and a BM to create the total field pattern. The residual-wave and BM radiation are both relatively strong in this case. Fig. 18 shows a contour plot of the normalized field (substrate voltage) for this case. It is interesting to note that inside the spectral-gap the residual wave assumes some of the character of a leaky-mode field. A curved, and somewhat distorted, pseudoleakage region evident in Fig. 18 exemplifies this fact. The curvature of the pseudoleakage region is more pronounced than in the $h/\lambda_0 = 0.08$ case of Fig. 15 (for which a physical leaky mode existed).

Moving further down in frequency, the final case studied in this paper is that for $h/\lambda_0 = 0.005$. In this low-frequency case, the operating point is well inside the spectral-gap region in the dispersion plot of Fig. 12. As a result of the low frequency, the continuous-spectrum current is very small, as shown in Fig. 19. The oscillations in the total current due to the interference between the BM and continuous-spectrum currents are still apparent although they are small in amplitude. This plot of the current components also shows definitively that this is a predominant BM case. Not surprisingly, the BM radiation field dominates the total radiated field, shown in Fig. 20, with only a slight downward magnitude shift due to the destructive interference

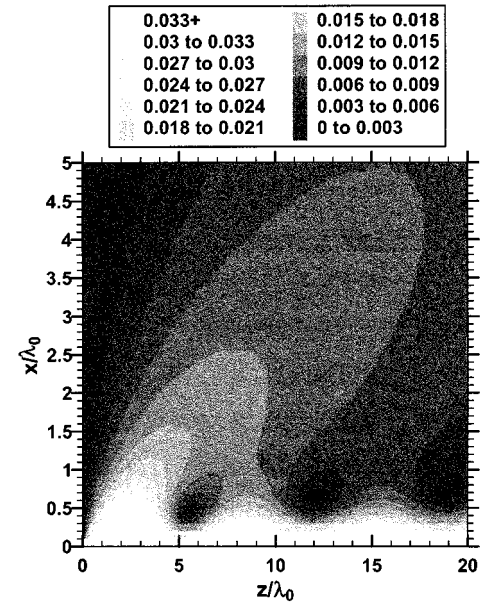

Fig. 18. Normalized substrate voltage (total) for the covered microstrip of Fig. 16.

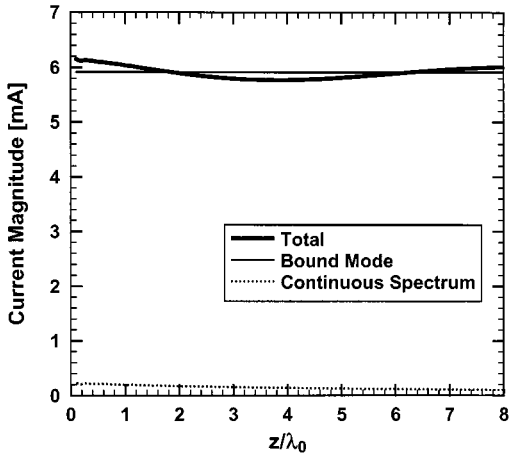

Fig. 19. Strip current magnitude for a covered microstrip ($h = 0.005\,\lambda_0$, $h_c = h$, $W = h$, and $\varepsilon_r = 2.2$) with a 1-[V] gap source.

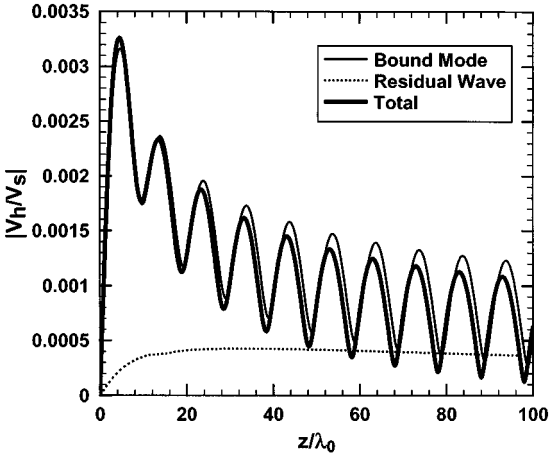

Fig. 20. Normalized substrate voltage for the covered microstrip of Fig. 19 at $x = \lambda_0$.

between the BM and residual-wave fields. The interference pattern in the BM field is evident, and as in the previous two cases,

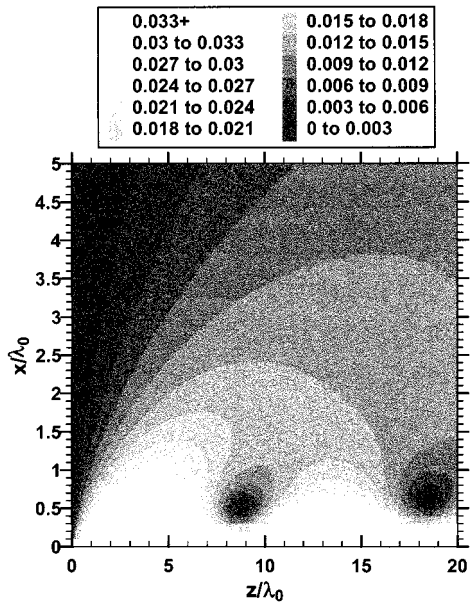

Fig. 21. Normalized substrate voltage (total) for the covered microstrip of Fig. 19.

the transverse distance is already large enough at $x = \lambda_0$ so the BM source-discontinuity radiation is larger than the infinite-line BM field. Since there is no physical leaky mode, and because the residual-wave field is so weak, there is no evidence of even a weakly defined pseudo-leakage region in the contour plot of the total radiated field shown in Fig. 21. The total radiated field is almost identical to that of the BM radiation field.

IV. Conclusion

Four examples of covered microstrip lines have been examined to study the radiated fields (fields radiated into the parallel-plate structure) due to the currents induced by a finite-gap source. For these four examples, the currents on the line have the following characteristics: a BM together with a predominant leaky mode, a BM together with equally-strong leaky-mode and residual-wave currents, a BM together with a significant residual-wave current, and no physical leaky mode, and a predominant BM with no physical leaky mode and little residual-wave current. The results presented for these four examples led to some unexpected general conclusions.

In all of the cases, the BM radiation field possesses an interesting interference pattern along the length of the microstrip line close to the strip, created by the interaction of an infinite-line BM field and a BM source-discontinuity radiation field. For covered microstrip structures that support a strong physical leaky mode, the radiation from the line current is predominantly due to leakage when the observation point is near the source, and close to the angle of leakage. However, when the observation point is outside the leakage region and further from the source, the radiation field—although weaker—is primarily due to BM discontinuity radiation. Interestingly, for structures that have a nonphysical leaky mode and a relatively strong residual wave, a strong region of directed radiation may also be observed. In these cases the residual-wave field partially assumes the role of the leaky-mode field, thus creating a similar total radiation pattern even though the residual wave itself is not a guided mode on the structure.

Another interesting observation is that the radiation field of the leaky-mode current is usually not the strongest at the source location, even though the leaky-mode current is strongest there. Instead, the leaky-mode radiation field is typically strongest at a distance of several wavelengths down the line from the source. The leaky-mode radiation field appears to effectively emanate from this location, at a leakage angle that is determined by the phase constant of the leaky mode.

Appendix

Here, a derivation of the parallel-plate excitation coefficient A in (9) is given, using the spectral-domain immitance (SDI) method [17], [18].

The general expression for the TM_y magnetic vector potential of the dominant TM_0 parallel-plate mode within the substrate due to a unit-amplitude z-directed infinitesimal dipole located at $y = h$ is

$$A_y^{pp}(x, y, z) = C\cos(\phi)\, H_1^{(2)}(k_{pp}\rho)\cos(k_{y1}y) \tag{A1}$$

where ϕ and ρ denote the usual polar coordinates, with angle ϕ measured from the z axis (instead of the x axis). The normalized (unity at $y = 0$) function $\cos(k_{y1}y)$ describes the vertical variation of the magnetic vector potential (or the vertical electric field) in the substrate. The complete equation for the vertical variation of the vertical electric field between the parallel plates is given in (10). The SDI method is used to first solve for the unknown constant C, and, from this, the constant A is determined.

In the SDI method [17], [18], a rotated rectangular coordinate system is used where the u and v directions are rotated away from the z and x axes by an angle $\overline{\phi}$. Following the SDI method [17], [18], the u component of the transformed transverse electric field is modeled as voltage on the TM transmission-line equivalent circuit and is given in terms of the transformed surface current of the source as

$$\tilde{E}_u = V^{\mathrm{TM}} = V_i^{\mathrm{TM}}(k_t)\left[-\tilde{\mathbf{J}}_s \cdot \hat{\mathbf{u}}\right] = V_i^{\mathrm{TM}}(k_t)\left[-\tilde{J}_{sz}\frac{k_z}{k_t}\right] \tag{A2}$$

where V_i^{TM} is the voltage on the transmission-line model due to a shunt 1-A current source at $y = h$ (the location of the surface current), and $k_t = (k_x^2 + k_y^2)^{1/2}$. Since the source in this configuration is a z-directed unit-amplitude dipole, the transform of the current density is unity. Thus, (A2) becomes

$$\tilde{E}_u = -V_i^{\mathrm{TM}}(k_t)\frac{k_z}{k_t}. \tag{A3}$$

The u component of the transformed field can be written as

$$\tilde{E}_u = -\frac{k_t}{\omega\mu_1\varepsilon_1}\frac{\partial \tilde{A}_y}{\partial y}. \tag{A4}$$

Equating (A3) and (A4), solving for $\partial\tilde{A}_y/\partial y$, and applying the inverse Fourier transform, it is found that

$$\frac{\partial A_y}{\partial y} = \frac{1}{(2\pi)^2}\int_{-\infty}^{+\infty}\int_{-\infty}^{+\infty}\frac{\omega\mu_1\varepsilon_1 k_z}{k_t^2}\,V_i^{\mathrm{TM}}(k_t) \cdot e^{-j(k_x x+k_z z)}\,dk_x\,dk_z. \quad \text{(A5)}$$

Converting to polar coordinates, (A5) can be written as

$$\frac{\partial A_y}{\partial y} = \frac{j\omega\mu_1\varepsilon_1}{(2\pi)^2}\frac{\partial}{\partial z}\int_0^{2\pi}\int_0^{\infty}\frac{V_i^{\mathrm{TM}}(k_t)}{k_t} \cdot e^{-jk_t\rho\cos(\phi-\overline{\phi})}\,dk_t\,d\overline{\phi}. \quad \text{(A6)}$$

The integral over $\overline{\phi}$ can be performed analytically, yielding the J_0 Bessel function, so that (A6) simplifies to

$$\frac{\partial A_y}{\partial y} = \frac{j\omega\mu_1\varepsilon_1}{2\pi}\frac{\partial}{\partial z}\int_0^{\infty}\frac{V_i^{\mathrm{TM}}(k_t)}{k_t}\,J_0(k_t\rho)\,dk_t. \quad \text{(A7)}$$

Writing the J_0 Bessel function in (A8) in terms of the corresponding Hankel functions, and using symmetry, it follows that

$$\frac{\partial A_y}{\partial y} = \frac{j\omega\mu_1\varepsilon_1}{4\pi}\frac{\partial}{\partial z}\int_{-\infty}^{+\infty}\frac{V_i^{\mathrm{TM}}(k_t)}{k_t}\,H_0^{(2)}(k_t\rho)\,dk_t. \quad \text{(A8)}$$

The field of the TM_0 parallel-plate mode can be obtained by replacing the total field by the residue contribution from the TM_0 pole. Doing this, and noting that

$$\frac{\partial}{\partial z}\left\{H_0^{(2)}(k_{pp}\rho)\right\} = -H_1^{(2)}(k_{pp}\rho)k_{pp}\cos(\phi) \quad \text{(A9)}$$

the derivative of the magnetic vector potential for the TM_0 parallel-plate mode is

$$\frac{\partial A_y^{pp}}{\partial y} = -\frac{\omega\mu_1\varepsilon_1}{2}\,\mathrm{Res}\left\{V_i^{\mathrm{TM}}(k_{pp})\right\}H_1^{(2)}(k_{pp}\rho)\cos(\phi) \quad \text{(A10)}$$

where "Res" denotes residue. Comparing with (A1), and noting that the derivative of $\cos(k_{y1}y)$ at $y = h^-$ is $-k_{y1}\sin(k_{y1}h)$, it is found that

$$C = \frac{\omega\mu_1\varepsilon_1}{2\,k_{y1}\sin(k_{y1}h)}\,\mathrm{Res}\left\{V_i^{\mathrm{TM}}(k_{pp})\right\}. \quad \text{(A11)}$$

The vertical electric field in the substrate can now be calculated using [19]

$$E_y^{pp} = \frac{1}{j\omega\mu_1\varepsilon_1}\left(k_1^2+\frac{\partial}{\partial y^2}\right)A_y^{pp} = \frac{1}{j\omega\mu_1\varepsilon_1}\,(k_{pp}^2)A_y^{pp}. \quad \text{(A12)}$$

Hence,

$$A = \frac{k_{pp}^2 C}{j\omega\mu_1\varepsilon_1} = \frac{k_{pp}^2}{j\,2\,k_{y1}\sin(k_{y1}h)}\,\mathrm{Res}\left\{V_i^{\mathrm{TM}}(k_{pp})\right\}. \quad \text{(A13)}$$

The voltage term V_i^{TM} can be found by analyzing the transmission line circuit that models the parallel-plate structure in Fig. 1. Assuming a 1-A current source, this voltage is simply the input impedance seen by the parallel current source at $y = h$, given by

$$V_i^{\mathrm{TM}}(k_t) = \frac{j}{Y_1^{\mathrm{TM}}\cot(k_{y1}h) + Y_0^{\mathrm{TM}}\cot(k_{y0}h)} \quad \text{(A14)}$$

where

$$Y_n^{\mathrm{TM}} = \frac{\omega\varepsilon_n}{k_{yn}}$$

$$k_{yn} \equiv \sqrt{k_n^2 - k_t^2},$$

with n either 0 or 1. The residue term in (A13) may be calculated numerically from (A14), once the pole location of k_{pp} has been determined.

REFERENCES

[1] D. Nghiem, J. T. Williams, D. R. Jackson, and A. A. Oliner, "Proper and improper dominant mode solutions for stripline with an air gap," *Radio Sci.*, vol. 28, no. 6, pp. 1163–1180, Nov.–Dec. 1993.

[2] ——, "Existence of a leaky dominant mode on microstrip line with an isotropic substrate: Theory and measurements," *IEEE Trans. Microwave Theory Tech.*, vol. 44, pp. 1710–1715, Oct. 1996.

[3] M. Tsuji, H. Shigesawa, and A. A. Oliner, "Printed-circuit waveguide with anisotropic substrates: A new leakage effect," in *Proc. IEEE MTT-S Int. Microwave Symp. Dig.*, 1989, pp. 783–786.

[4] ——, "Simultaneous propagation of both bound and leaky modes on conductor-backed coplanar strips," in *Proc. IEEE MTT-S Int. Microwave Symp. Dig.*, Atlanta, GA, 1993, pp. 1295–1298.

[5] H. Shigesawa, M. Tsuji, and A. A. Oliner, "Conductor-backed slot line and coplanar waveguide: Dangers and full-wave analysis," in *Proc. IEEE MTT-S Int. Microwave Symp. Dig.*, 1988, pp. 199–202.

[6] J. Zehentner and J. Machac, "Properties of CPW in the sub-mm wave range and its potential to radiate," in *Proc. IEEE MTT-S Int. Microwave Symp. Dig.*, 2000, pp. 1061–1064.

[7] C. DiNallo, F. Mesa, and D. R. Jackson, "Excitation of leaky modes on multiplayer stripline structures," *IEEE Trans. Microwave Theory Tech.*, vol. 46, pp. 1062–1071, Aug. 1998.

[8] H. Shigesawa, M. Tsuji, and A. A. Oliner, "The nature of the spectral-gap between bound and leaky solution when dielectric loss is present in printed-circuit lines," *Radio Sci.*, vol. 28, no. 6, pp. 1235–1243, Nov.–Dec. 1993.

[9] D. P. Nyquist and D. J. Infante, "Discrete higher-order leaky-wave modes and the continuous spectrum of stripline," *IEICE Trans.*, vol. E78-C, pp. 1331–1338, Oct. 1995.

[10] J. M. Grimm and P. P. Nyquist, "Spectral analysis considerations relevant to radiation and leaky modes of open-boundary microstrip transmission line," *IEEE Trans. Microwave Theory Tech.*, vol. 41, pp. 150–153, Jan. 1993.

[11] D. R. Jackson, F. Mesa, M. J. Freire, D. P. Nyquist, and C. DiNallo, "An excitation theory for bound modes, leaky modes, and residual-wave currents on stripline structures," *Radio Sci.*, vol. 35, no. 2, pp. 495–510, Mar.–Apr. 2000.

[12] F. Mesa, A. A. Oliner, D. R. Jackson, and M. J. Freire, "The influence of a top cover on the leakage from microstrip line," *IEEE Trans. Microwave Theory Tech.*, vol. 48, pp. 2240–2248, Dec. 2000.

[13] J. L. Cina and L. Carin, "Mode conversion and leaky-wave excitation at open-end coupled-microstrip discontinuities," *IEEE Trans. Microwave Theory Tech.*, vol. 43, pp. 2066–2071, Sept. 1995.

[14] N. K. Das, "Power leakage, characteristic impedance, and leakage-transition behavior of finite-length stub sections of leaky printed transmission lines," *IEEE Trans. Microwave Theory Tech.*, vol. 44, pp. 526–536, Apr. 1996.

[15] C. M. Bender and S. A. Orszag, *Advanced Mathematical Methods for Scientists and Engineers*. New York: McGraw-Hill, 1978, pp. 369–375.

[16] F. J. Villegas, D. R. Jackson, J. T. Williams, and A. A. Oliner, "Leakage fields from planar semi-infinite transmission lines," *IEEE Trans. Microwave Theory Tech.*, vol. 47, no. 4, pp. 443–454, Apr. 1999.

[17] T. Itoh, "Spectral domain immitance approach for dispersion characteristics of generalized printed transmission lines," *IEEE Trans. Microwave Theory and Tech.*, vol. MTT-28, pp. 733–736, June 1980.

[18] ——, *Numerical Techniques for Microwave and Millimeter-Wave Passive Structures*. New York: Wiley, 1989, pp. 334–351.

[19] R. F. Harrington, *Time-Harmonic Electromagnetic Fields*. New York: McGraw-Hill, 1961, pp. 143–155.

William L. Langston (S'95) was born in Houston, TX, on September 30, 1975. He received the B.S.E.E. (*magna cum laude*) and M.S.E.E. degrees from the University of Houston, Houston, TX, in 1999 and 2001, respectively, and is currently working toward the Ph.D. degree in electrical engineering at the University of Houston.

From 1999 to 2001, he was a Research Assistant in the Department of Electrical and Computer Engineering, University of Houston. His research interests include leakage effects in microwave integrated circuits, bioelectromagnetics, computational electromagnetics, and adaptive antenna arrays.

Jeffery T. Williams (S'85–M'87–SM'97) was born in Maui, HI, on July 24, 1959. He received the B.S., M.S., and Ph.D. degrees in electrical engineering from the University of Arizona, Tucson, in 1981, 1984, and 1987, respectively.

In 1987, he joined the Department of Electrical and Computer Engineering, University of Houston, Houston, TX, where he is currently an Associate Professor. Prior to that, he was a Schlumberger-Doll Research Fellow at the University of Arizona. He spent four summers (1983–1986) at the Schlumberger-Doll Research Center, Ridgefield, CT, as a Research Scientist. From 1981 to 1982, he was a Design Engineer at the Zonge Engineering and Research Organization, Tucson, AZ, and a Summer Engineer at the Lawrence Livermore National Laboratory, Livermore, CA. His research interests include the design and analysis of high-frequency antennas and circuits, high-frequency measurements, the application of high-temperature superconductors and leaky-wave propagation. He was an Associate Editor for *Radio Science*.

Dr. Williams is a member of URSI Commission B. He was an associate editor for the IEEE TRANSACTIONS ON ANTENNAS AND PROPAGATION.

David R. Jackson (S'83–M'84–SM'95–F'99) was born in St. Louis, MO, on March 28, 1957. He received the B.S.E.E. and M.S.E.E. degrees from the University of Missouri, Columbia, in 1979 and 1981, respectively, and the Ph.D. degree in electrical engineering from the University of California at Los Angeles, in 1985.

From 1985 to 1991, he was an Assistant Professor in the Department of Electrical and Computer Engineering, University of Houston, Houston, TX. From 1991 to 1998, he was an Associate Professor in the same department, and since 1998, he has been a Professor in the same department. His current research interests include microstrip antennas and circuits, leaky-wave antennas, leakage and radiation effects in microwave integrated circuits, periodic structures, and bioelectromagnetics. He is an Associate Editor for the *International Journal of RF and Microwave Computer-Aided Engineering* and is a past Associate Editor for *Radio Science*.

Dr. Jackson is the chapter activities coordinator for the IEEE Antennas and Propagation Society (IEEE AP-S) and the chair of the Technical Activities Committee for URSI, U.S. Commission B. He is a distinguished lecturer for the IEEE AP-S. He is a past associate editor for the IEEE TRANSACTIONS ON ANTENNAS AND PROPAGATION. He was a member of the IEEE AP-S AdCom.

Francisco Mesa (M'94) was born in Cadiz, Spain, in April 1965. He received the Licenciado and Ph.D. degrees in physics from the University of Seville, Seville, Spain, in 1989 and 1991, respectively.

He is currently an Associate Professor in the Department of Applied Physics, University of Seville. His research interests focus on electromagnetic propagation/radiation in planar lines with general anisotropic materials.